Biophysical Chemistry 18 (1983) 101–109
Elsevier

BPC 00793

EFFICIENCY OF ENERGY CONVERSION IN MODEL BIOLOGICAL PUMPS

OPTIMIZATION BY LINEAR NONEQUILIBRIUM THERMODYNAMIC RELATIONS

Jörg W. STUCKI [a], Mario COMPIANI [a] and S. Roy CAPLAN [b]

[a] *Pharmakologisches Institut der Universität Bern, Bern, Switzerland, and* [b] *Department of Membrane Research, The Weizmann Institute of Science, Rehovot, Israel*

Received 9th December 1982
Accepted 1st May 1983

Key words: Efficiency; Optimization; Linearity; Nonlinearity; Feedback regulation; Evolutionary drive

Experimental investigations showed linear relations between flows and forces in some biological energy converters operating far from equilibrium. This observation cannot be understood on the basis of conventional nonequilibrium thermodynamics. Therefore, the efficiencies of a linear and a nonlinear mode of operation of an energy converter (a hypothetical redox-driven H^+ pump) were compared. This comparison revealed that at physiological values of the forces and degrees of coupling (1) the force ratio permitting optimal efficiency was much higher in the linear than in the nonlinear mode and (2) the linear mode of operation was at least 10^6-times more efficient that the nonlinear one. These observations suggest that the experimentally observed linear relations between flows and forces, particularly in the case of oxidative phosphorylation, may be due to a feedback regulation maintaining linear thermodynamic relations far from equilibrium. This regulation may have come about as the consequence of an evolutionary drive towards higher efficiency.

1. Introduction

The detailed experimental investigation of several biological energy converters, such as oxidative phosphorylation, mitochondrial H^+ pumps and $(Na^+ + K^+)$-ATPase, has revealed linear relations between flows and forces in a far-from-equilibrium regime which, where tested, exhibit symmetry suggestive of Onsager reciprocity [1–5]. This experimental observation is very astonishing, since it seems to be in sharp contrast to the severe restriction of linear relations to the immediate neighborhood of equilibrium. In fact, classical nonequilibrium thermodynamics furnishes the criterion for the validity of linear relations for processes involving chemical reactions in the form of the well known inequality $|X| \ll RT$, where X is a generalized force like a chemical affinity or an electrochemical transmembrane gradient [6,7]. (Of course, purely vectorial processes, in contrast to scalar processes, are notoriously linear when by the above criterion they are far from equilibrium, examples being Ohm's law, Poiseuille's law, etc.). In biological systems, therefore, the experimentally observed linearity seems not to be the natural consequence of a near-equilibrium regime but appears rather to be the result of a sophisticated feedback regulation which maintains linearity far from equilibrium. Obviously, such a postulate leads immediately to the question: what is the advantage for the system to obey linear laws between flows and forces? In other words, we have to answer the question as to whether the linearity of laws far from equilibrium is perhaps the result of some type of optimization. In this paper we will demonstrate that the efficiency of a rather general class of model biological energy converters driven far from equilibrium is greatly improved by linear relations between flows and forces.

It is important to stress that the comparison of

efficiencies of linear and nonlinear energy converters cannot be done solely on the basis of purely phenomenological thermodynamic schemes, but in contrast, necessitates a combination of thermodynamic and kinetic considerations. The requirement for kinetic considerations unfortunately leads to a loss of the generality characteristic of purely thermodynamic schemes, simply because kinetics is always based on specific models. However, the diagrammatic method of Hill [8] allows the introduction of kinetic considerations into thermodynamic schemes on a low level of detail. Therefore, a treatment of our problem within the framework of Hill's approach allows us to give an answer which is applicable to a broad class of biological energy converters. In addition to being quite general, Hill's method has the additional advantage of being elegant and chemically transparent.

In section 2 we will present a general model of noncooperative energy converters and section 3 will demonstrate the principle of optimization through linearity on the basis of this model.

2. The model

Most of the experimentally investigated biological energy-converting systems are active transport systems. A convenient description of representative systems of this type has been given by Hill [8]. Without loss of generality we can represent the basic features of such systems by the simple scheme shown in fig. 1a for the case of a hypothetical redox-driven H^+ pump (see also ref. 9). Different states of the transporting enzyme embedded in the membrane are represented in sketches 1–5. It should be noted that each of these states may consist of a large number of substates equilibrating with each other on a relatively fast time scale.

The kinetic description of the system in fig. 1a is given in fig. 1b. In this Hill diagram each line represents a possible transition among the different states depicted in fig. 1a. To be more specific, each line represents the conventional arrows for the forward and the backward reaction between the two states connected by the line. Hence, each line is implicitly associated with two first-order

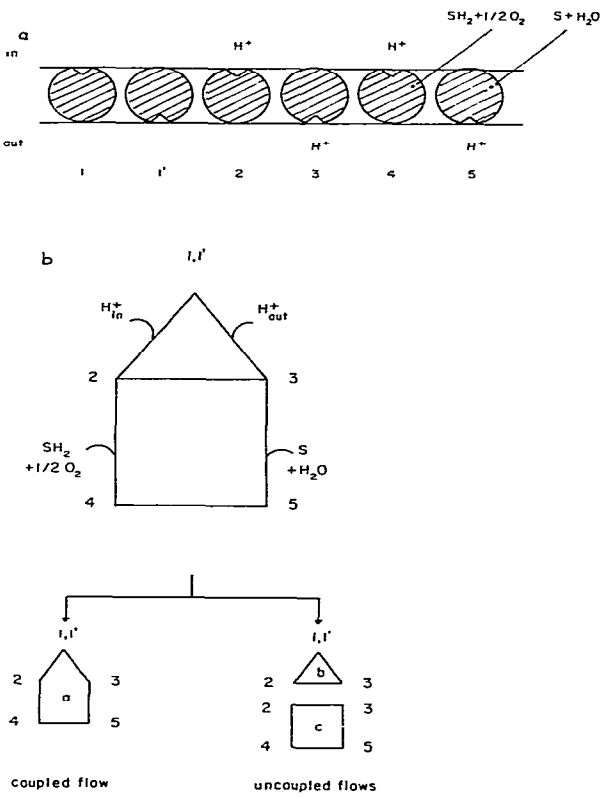

Fig. 1. (a) Model of a hypothetical redox H^+ pump. The H^+-transporting enzyme sits in a membrane in different configurations: empty H^+-binding site oriented towards the inside or outside compartment (states 1 and 1') and same configurations but with an H^+ bound to the H^+-binding site (states 2 and 3). For states 4 and 5 an arbitrary mechanistic choice is made. The reduced substrate SH_2 is bound to the configuration where the occupied H^+-binding site is oriented inwards (state 4). Oxidation of the substrate induces an obligatory conformational change of the enzyme such that the bound H^+ now faces the outside compartment (state 5). (b) Hill diagram of redox H^+ pump. Five kinetically relevant states of the H^+-transporting enzyme depicted in panel a are mapped on a linear graph (Hill diagram) as described in the text. There are three cycles labelled a, b and c which each permit an independent steady state with one degree of freedom of H^+ flow and/or redox reaction. Coupling of substrate oxidation to net H^+ transport is only possible in cycle a whereas cycles b and c permit uncoupled flows of either H^+ across the membrane or redox reaction, respectively. The overall steady state of the enzyme is represented by a linear combination of these three independent cycle flows.

rate constants. For convenience, without loss of generality, we assume the forward and backward transitions between states 1 and 1′ to be relatively rapid. This permits us to represent the system by five kinetically relevant states. Ligand binding to (or release from) the enzyme is also indicated.

Although we have represented the system by five states, the argument to be presented below would not be influenced at all by the introduction of any number of additional states, i.e., rate-determining transitions, providing the following requirements are satisfied: we do not introduce rate-determining transitions of 'naked' states between 1 and 1′, and the 'leakage' transition or chain of transitions occurs as an alternative to the binding of substrate. Relaxing the first requirement does not change the argument in its essentials. The diagram in fig. 1b is composed of three cycles. As has been shown by Hill, the net steady-state flows may be written in terms of these three cycle flows [8].

Thus

$$J_H = \text{cycle flow } a + \text{cycle flow } b \tag{1}$$

$$J_O = \text{cycle flow } a + \text{cycle flow } c \tag{2}$$

These equations take the following nonlinear explicit form which can be read off the diagrams according to a straightforward algorithm [8]

$$J_H^{n1} = n\left[(a+b)(e^{nX_H/RT}-1) + a(e^{X_O/RT}-1) + a(e^{nX_H/RT}-1)(e^{X_O/RT}-1)\right] \tag{3}$$

$$J_O^{n1} = a(e^{nX_H/RT}-1) + [a+c(1+\gamma)](e^{X_O/RT}-1) + (a+c)(e^{nX_H/RT}-1)(e^{X_O/RT}-1) \tag{4}$$

In these equations X_H and X_O represent the electrochemical potential difference of H^+ across the membrane and the redox potential applied to the pump [10], respectively, where n is the number of H^+ bound or released in the transitions 1–2 or 1–3. The quantities a, b and c are clusters of kinetic constants and concentrations, related to cycle diagrams a, b and c, respectively, having the following structure

$$a = (A/\Sigma)c_S(c_H^{ex})^n \tag{5}$$

$$b = (B/\Sigma)(c_H^{ex})^n \tag{6}$$

$$c = (C/\Sigma)c_S(c_H^{ex})^n \tag{7}$$

where c_S is the product (i.e., oxidized substrate) and c_H^{ex} the H^+ concentration on the external side (i.e., the side towards which pumping occurs). A, B and C contain first-order rate constants only and hence, for isothermal systems, are constants. Σ is a sum of 'directional diagrams', i.e., a sum of products of rate coefficients and associated concentrations taken along every possible path, or combination of paths, leading to each one of the states [8]. The parameter γ is a convenient measure for the relative binding affinity for H^+ on either side of the membrane. This parameter depends on the ratio of the external to the internal binding affinity.

In the near-equilibrium limit, eqs. 3 and 4 assume the conventional linear and symmetric form

$$J_H^1 = n^2(a+b)X_H/RT + anX_O/RT \tag{8}$$

$$J_O^1 = anX_H/RT + [a+c(1+\gamma)]X_O/RT \tag{9}$$

These equations readily permit a kinetic and intuitive interpretation of the degree of coupling q and the phenomenological stoichiometry Z [2,11]

$$q = \left\{\left[1+\frac{B}{Ac_S}\right]\left[1+\frac{C(1+\gamma)}{A}\right]\right\}^{-1/2} \tag{10}$$

$$Z = n\left\{\left[1+\frac{B}{Ac_S}\right]\Big/\left[1+\frac{C(1+\gamma)}{A}\right]\right\}^{1/2} \tag{11}$$

Note that the quantities q and Z depend on the state of the system as defined by the concentration c_S. Alternatively, the state of the system might be defined in terms of c_{SH_2} (see fig. 1b). For the special case $B = C = 0$ we obtain $q = 1$ and $Z = n$. This situation corresponds to the absence of any leakage flows. This clearly illustrates that the phenomenological stoichiometry Z is, in general, not equal to the mechanistic stoichiometry n.

The flow ratio [11] can be treated in a similar fashion by defining the state of the system in terms of c_S (or c_{SH_2}). Thus, we find that the flow ratio is a function of only the thermodynamic forces, being independent of Σ or the absolute values of A, B and C over the whole nonlinear range (Σ has canceled out and A, B and C appear only in ratios)

$$\left(\frac{J_H}{J_O}\right)^{n1} = n\left\{\left[\left(1+\frac{B}{Ac_S}\right)(e^{nX_H/RT}-1)+(e^{X_O/RT}-1)\right.\right.$$

$$+(e^{nX_H/RT}-1)(e^{X_O/RT}-1)\Big]$$
$$\times\left[(e^{nX_H/RT}-1)+\left(1+\frac{C[1+\gamma]}{A}\right)(e^{X_O/RT}-1)\right.$$
$$\left.+\left(1+\frac{C}{A}\right)(e^{nX_H/RT}-1)(e^{X_O/RT}-1)\Big]\right\}^{-1} \quad (12)$$

Similarly, for the linear range

$$\left(\frac{J_H}{J_O}\right)^{1}=n\frac{\left(1+\frac{B}{Ac_S}\right)nX_H+X_O}{nX_H+\left(1+\frac{C[1+\gamma]}{A}\right)X_O} \quad (13)$$

Therefore, the efficiency [9] can also be described throughout the nonlinear range by

$$\eta^{nl}=-\left(\frac{J_H}{J_O}\right)^{nl}\frac{X_H}{X_O} \quad (14)$$

and for the linear range

$$\eta^{l}=-\left(\frac{J_H}{J_O}\right)^{l}\frac{X_H}{X_O} \quad (15)$$

In what follows, we compare the behavior of a system in two modes: one following the nonlinear relationship, eqs. 3 and 4, and the other constrained in some manner to follow the linear relationship, eqs. 8 and 9, for all values of the forces $X_H<0$ and $X_O>0$ even far from equilibrium. By virtue of the definition of q and Z common to both modes, this comparison can be made in a physically consistent manner.

It is important to realize that as a corollary of eqs. 10 and 11 we have the following identities:

$$\frac{B}{Ac_S}\equiv\frac{Z}{nq}-1,\quad \frac{C(1+\gamma)}{A}\equiv\frac{n}{qZ}-1.$$

Thus, it is seen on examining eq. 12 that the behavior of the flow ratio over the entire range from equilibrium to far from equilibrium is governed solely by q, Z, γ and n. The quantities q, Z and γ are kinetic parameters which depend only on the rate constants and, in the case of q and Z, on a single concentration – the concentration of the oxidized substrate. We have assumed that this concentration may be taken to be constant. This is not a heavy assumption – it simply means that we manipulate the substrate concentration when we move the system from near equilibrium to far from equilibrium just as is commonly done in a Michaelis-Menten analysis. The rate constants of the system do not vary, and neither does the mechanistic stoichiometry n. Hence, q, Z, γ and n are constant kinetic parameters independent of whether the system is near or far from equilibrium. Any self-consistent set of rate constants for the model, i.e., any set satisfying the condition of microscopic reversibility, will generate values of q and Z which satisfy the thermodynamic criterion $-1\le q\le 1$ and a kinetic limitation on Z discussed below. Hence, whole classes of models may be characterized kinetically by an a priori choice of q, Z, γ and n.

3. Comparison of efficiencies of the linear and nonlinear modes: optimization through linearity

A convenient measure for the deviation of the phenomenological from the mechanistic stoichiometry is the reduced phenomenological stoichiometry

$$\zeta=\frac{Z}{n} \quad (16)$$

This parameter is subject to the kinetic limitation

$$\frac{1}{q}\ge\zeta\ge q \quad (17)$$

(in our model q has a positive value).

The upper and lower boundaries are mathematical limits arising from $C=0$ and $B=0$, respectively. These limits could not be, in fact, reached by kinetic systems without violating the principle of microscopic reversibility.

It is, nevertheless, very instructive to consider the flow ratio at these boundaries in order to obtain an insight into the energy converter operating in either the linear or the nonlinear mode. At the upper boundary, i.e., at $\zeta=1/q$, we have

$$\left(\frac{J_H}{J_O}\right)^{nl}_{\zeta=1/q}=n\left[1+(\zeta^2-1)\frac{e^{nX_H/RT}-1}{e^{(nX_H+X_O)/RT}-1}\right] \quad (18)$$

and

$$\left(\frac{J_H}{J_O}\right)^{l}_{\zeta=1/q}=n\left[\frac{\zeta^2nX_H+X_O}{nX_H+X_O}\right] \quad (19)$$

By remembering that for a positive cycle flow in cycle a the second law imposes the restriction $nX_H + X_O > 0$ for not fully coupled systems [8], a straightforward calculation shows that [12]

$$\left(\frac{J_H}{J_O}\right)^{nl}_{\zeta=1/q} > \left(\frac{J_H}{J_O}\right)^{l}_{\zeta=1/q} \tag{20}$$

On the other hand, at the lower boundary, i.e., at $\zeta = q$, we have

$$\left(\frac{J_H}{J_O}\right)^{nl}_{\zeta=q} = (1+\gamma)\zeta^2 n\{[e^{(nX_H+X_O)/RT}-1] \times [(\zeta^2-1)(e^{nX_H/RT}-\gamma e^{X_O/RT}) + e^{(nX_H+X_O)/RT}(1+\zeta^2\gamma)-(\zeta^2+\gamma)]\}^{-1} \tag{21}$$

and

$$\left(\frac{J_H}{J_O}\right)^{l}_{\zeta=q} = n\left[\frac{nX_H+X_O}{nX_H+X_O/\zeta^2}\right] \tag{22}$$

A somewhat involved proof shows that for $\gamma \geqslant 1$ [12]

$$\left(\frac{J_H}{J_O}\right)^{nl}_{\zeta=q} < \left(\frac{J_H}{J_O}\right)^{l}_{\zeta=q} \tag{23}$$

By invoking the definition of the efficiencies, eqs. 14 and 15, we can summarize the conclusions from these inequalities in the form of the following theorem:

For $\gamma \geqslant 1$ we have

$$\eta^{nl} > \eta^{l} \quad \text{for} \quad \zeta = \frac{1}{q} \tag{24}$$

$$\eta^{nl} < \eta^{l} \quad \text{for} \quad \zeta = q$$

From this theorem it is obvious that there exists a value of ζ in the open interval $1/q > \zeta > q$ at which the efficiencies of the energy converter operating in the linear and in the nonlinear mode break even. In other words, there exist values for ζ where the energy converter operates more efficiently in either the linear or the nonlinear mode. Note that a fully coupled system is characterized by a trivial break-even point only since $q = \zeta = 1$ due to $B = C = 0$. Therefore, in a fully coupled system the efficiencies of both the linear and nonlinear mode of operation are always equal. Since it has been shown, however, that $q = 1$ is incompatible with optimal efficiency in biological energy converters operating at nonvanishing output flows [2], this special case is of little physiological interest.

The explicit calculation of the break-even point in the interval $1/q > \zeta > q$ is analytically quite complicated. Therefore, we have calculated this point numerically in what follows. With this procedure our analysis will inevitably be limited to arbitrarily selected values of the parameters. However, there will be no severe loss of generality, since our theorem stated above guarantees the existence of a break-even point for all values $q < 1$ as discussed, at least for $\gamma \geqslant 1$.

The major problem we are now concerned with is the exact location of the break-even point for physiologically meaningful values of the parameters. To be more specific, we would like to known whether the linear or the nonlinear mode of operation of the converter is more efficient within the physiological range of the parameters. Apart from this qualitative criterion we would also like to obtain a quantitative estimate of the efficiency gained by switching from a nonlinear to a linear mode of operation. For this it is convenient to introduce a measure for the efficiency gain in the form of the ratio

$$\rho = \eta^{l}/\eta^{nl} \tag{25}$$

Note that the break-even point is characterized by $\rho = 1$.

Before calculating this ratio let us first consider a general feature of the nonlinear mode. Fig. 2 depicts the dependence of the efficiency η^{nl} on the force ratio $x = ZX_H/X_O$ as well as on the input force X_O. From this figure it readily appears that, in contrast to the linear mode, the efficiency of the nonlinear mode explicitly depends on the magnitude of the input force X_O except at the level-flow state [11], i.e., at $x = 0$. In fact, at level flow we obtain the straightforward result

$$\left(\frac{J_H}{J_O}\right)^{nl}_{lf} = \left(\frac{J_H}{J_O}\right)^{l}_{lf} = qZ \tag{26}$$

irrespective of X_O for all values of $1/q > \zeta > q$. However, the efficiency vanishes at the level-flow state, since $X_H = 0$ (see eqs. 14 and 15). Therefore, level flow is a trivial break-even point of the

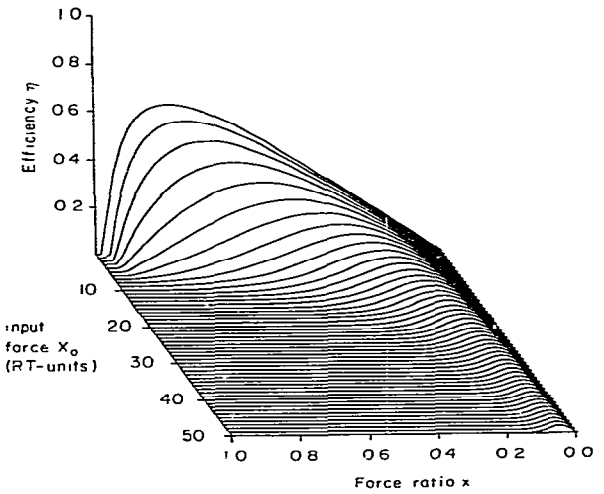

Fig. 2. Efficiency surface of nonlinear mode of energy converter. The efficiency of the nonlinear mode of the energy converter η^{nl} was calculated from eqs. 12 and 14 and was plotted vs. the force ratio x for the different values of the input force X_O shown in the figure. Upon increasing X_O the absolute magnitude of optimal efficiency η^{nl}_{opt} decreases and the optimal force ratio x^{nl}_{opt} is shifted toward level flow, i.e., $x = 0$. This behavior is in contrast to the linear mode of the energy converter where both η^{l}_{opt} and x^{l}_{opt} are independent of X_O. Parameters used for this calculation: $q = q_p^{cc} = 0.972$ (see ref. 2) and $Z = 2.83$, $n = 3$, $\gamma = 1.1$.

system which is of no practical interest. The explicit dependence of η^{nl} on X_O is further illustrated by the fact that for the linear mode the optimal efficiency only depends on q [11]:

$$\eta^{l}_{opt} = \left(\frac{q}{1+\sqrt{1-q^2}} \right)^2 \tag{27}$$

The corresponding quantity η^{nl}_{opt} for the nonlinear mode, however, shows a complicated dependence on X_O in addition to q. The same feature holds for the value of the force ratio permitting optimal efficiency. For the linear mode we have that

$$x^{l}_{opt} = -\frac{q}{1+\sqrt{1-q^2}} \tag{28}$$

which is a function of q only. The corresponding quantity x^{nl}_{opt} for the nonlinear mode in addition to q also depends on X_O.

As emerges from fig. 2, this dependence on X_O has the consequence that the efficiency of the nonlinear mode drops to low values at high values of X_O. Furthermore, at high values of X_O the value of x^{nl}_{opt} is shifted towards level flow. These consequences are of an immediate practical interest for biological energy converters.

In fig. 3 the values of x^{nl}_{opt} are plotted vs. X_O for four physiologically meaningful degrees of coupling. Briefly, the degrees of coupling q_f and q_p maximize net output flow and output power at η^{l}_{opt}, respectively [2]. The values q_f^{cc} and q_p^{cc} are the corresponding economic counterparts which, in addition, minimize the energy costs of energy transformation. As readily appears from the plot in fig. 3 x^{nl}_{opt} approaches zero at high input forces. In the overall process of oxidative phosphorylation, for example, which certainly represents the most important energy converter in aerobic tissue, the input force is the redox potential of the oxidiz-

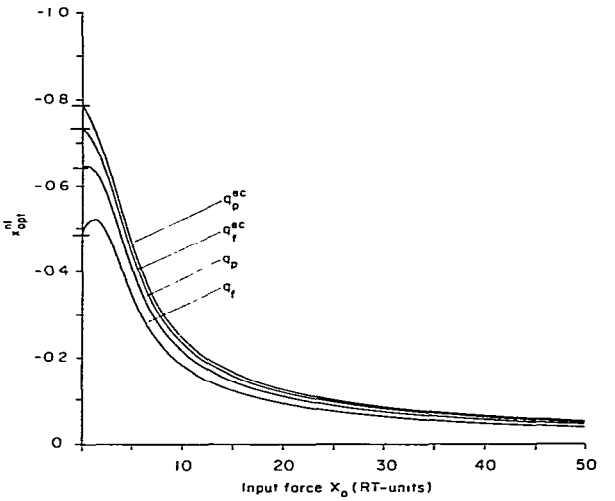

Fig. 3. Optimal force ratio of the nonlinear mode of the energy converter. The force ratios x^{nl}_{opt} corresponding to optimal efficiencies of the nonlinear mode of the energy converter η^{nl}_{opt} were searched numerically by using eqs. 12 and 14 for each value of X_O and for the four degrees of coupling q indicated in the figure. These values were then plotted vs. the input force X_O. Parameters used for this calculation: $q_f = 0.786$, $q_p = 0.910$, $q_f^{cc} = 0.953$ and $q_p^{cc} = 0.972$ (see text and ref. 2), $Z = 2.83$, $n = 3$, $\gamma = 1.1$.

able substrates whereas the output force is the phosphate potential by which the majority of energy-utilizing processes in the cell are driven [2]. It is sometimes claimed that in vivo these two forces are essentially balanced, so that the system operates close to (or at) reversible equilibrium. However, this could only be true if the system were completely coupled ($q = 1$), in which case the two processes would merge into a single process governed by a single total force that might be very small or zero. Since we know that in mitochondria $q < 1$ (see, for example, ref. 2), we cannot describe mitochondrial oxidative phosphorylation as a single process, and hence the above claim is invalid. From the fact that in this converter the input force is well above 50 RT units, it becomes clear that the nonlinear mode of operation of oxidative phosphorylation could only give rise to phosphate potentials of the order of a few RT units. As is well known from the work of the Brussels school, the self-organization of nonequilibrium systems and especially the onset and maintenance of macroscopic order and coherence characteristic for living organisms necessitate, however, considerable distance from equilibrium of the phosphate potential [13,14]. In the light of these considerations, the low phosphate potential resulting from a nonlinear mode of operation of oxidative phosphorylation seems hardly to be compatible with the very phenomenon of life. In contrast, the linear mode of operation of oxidative phosphorylation is not subject to such an unfavorable behavior, since x^{l}_{opt} does not depend on X_O (see eq. 28). This already shows that the linear mode of operation of energy converters should be strongly favored in biological systems.

This advantageous performance of the linear mode appears even more dramatically when calculating the gain ratio ρ as defined in eq. 25. In order to make this calculation, one has to choose a reference force ratio where the efficiencies of the two modes should be compared. It appears natural to make this comparison at x^{l}_{opt} for any degree of coupling (see eq. 28). This choice is also inspired by the fact, that for example in the liver cell, the force ratio x^{l}_{opt} appears to be a natural steady-state force ratio of oxidative phosphorylation [2]. Recent studies have indicated that this state is not only the result of an adaptation of oxidative phosphorylation to different metabolic conditions but that, moreover, this steady state is stabilized against fluctuations through thermodynamic buffering reactions catalyzed by enzymes especially designed for this purpose [15]. In fig. 4 the loci of different values of ρ calculated at x^{l}_{opt} are plotted in the q-X_O plane. From this figure it becomes quite clear that the loci of the break-even points, i.e., $\rho = 1$, are already reached at small input forces, especially at high values of q. In the physiologically meaningful range of the parameters, i.e., $0.8 < q < 1$ and $X_O > 40\ RT$ units, the linear mode exhibits a spectacular gain in efficiency as indicated by the contours of ρ around 10^6. This finding again indicates that selection pressure might well have favored the evolution towards a linear mode of operation of biological energy converters.

As a final illustration of the advantage to be

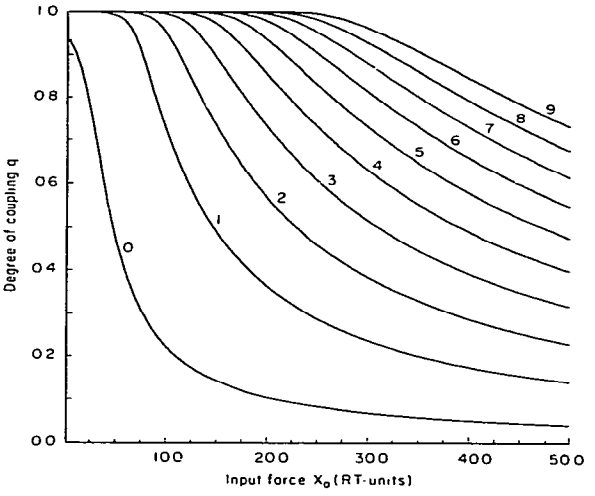

Fig. 4. Optimization of efficiency through linearity. The values of q yielding different discrete values of the gain ratio $\rho = \eta^{l}/\eta^{nl}$ (eq. 25) were calculated numerically from eqs. 12–15 at the reference force ratios x^{l}_{opt} (eq. 28). The loci for equal values of ρ were then plotted in the X_O-q plane for the values log $\rho = 0, 1, 2, \ldots, 9$ as indicated in the figure, the choice of parameters being $Z = 2.83$, $n = 3$ and $\gamma = 1.1$. From this plot it becomes evident that at high values of the input force X_O and within the physiological range of q the efficiency of the linear mode is superior to the efficiency of the nonlinear mode by a factor which approaches at least 10^6.

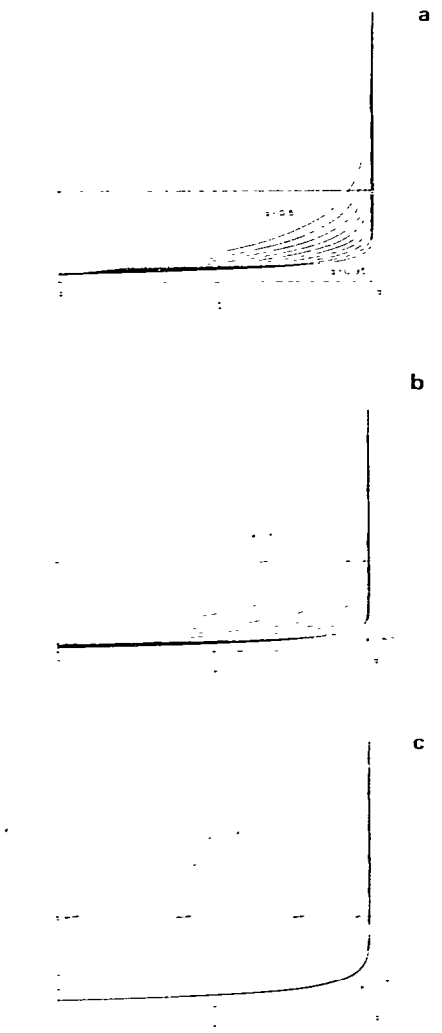

Fig. 5. Ratio of optimal efficiencies as a function of all kinetic parameters. Eqs. 10–12 and 14 were used to find η^{nl}_{opt} for any given set of kinetic parameters by numerical iteration. Eq. 27 then allowed calculation of the ratio of optimal efficiencies $\eta^{nl}_{opt}/\eta^{l}_{opt}$. This ratio was plotted as a function of ζ within its whole domain of definition given by eq. 17. In each panel a–c one parameter was varied while the others were kept fixed. (a) Variation of q from 0.5 to 0.95 in steps of 0.05. Fixed parameters: $X_O = 25\ RT$ units, $\gamma = 1.1$. (b) Variation of X_O from 5 to 50 RT units in steps of 5 RT units. Fixed parameters: $q = q_f = 0.786$, $\gamma = 1.1$. (c) Variation of γ from 10^3 to 10^{-6} in steps of 10^{-1}. Fixed parameters: $X_O = 25\ RT$ units, $q = q_f = 0.786$. The curves for $\gamma = 10$, 10^2 and 10^3 were indistinguishable.

gained by linearization, we consider the efficiency ratio $\eta^{nl}_{opt}/\eta^{l}_{opt}$. For any given values of the kinetic parameters and the input force, the maximal efficiency in the entire nonlinear range, η^{nl}_{opt}, may be computed and compared with the maximum efficiency in the linear range, η^{l}_{opt}, which depends only on the kinetic parameter q. In this comparison the force ratios are in generai quite different at the two optima. Fig. 5 shows that over an extraordinarily wide spectrum of models the ratio of maximal efficiencies given above is less than unity, and it clearly falls to very low values under physiological conditions. It should be borne in mind that q and $1/q$ are hypothetical limits which ζ cannot actually reach. It is seen that the highest values of input force, q and γ are associated with the lowest values of the ratio at all points on the ζ-coordinate. Note that in panel b and c the value chosen for q is q_f [2], a conservative lower estimate. The quantity γ may be expected to be in the vicinity of unity in the case under consideration; in the case of the Na^+ pump, where the external binding affinity is much lower than the initial binding affinity, it may have a value of the order of 10^{-2} [16].

In the light of these results it can be postulated that the experimentally observed linearity of the several biological energy converters operating far from equilibrium, as mentioned in section 1, appears not to be the natural consequence of a near-equilibrium regime, but rather to be due to an enzymatic feedback regulation. One way in which this might be realized would be through changes in state parameters [16]. For example, in the present context this would require appropriate modulation of the concentration of the oxidized substrate. Hence, linearity may well emerge as a result of compensatory nonlinear processes – indeed this must be the case in frog skin [17]. One might speculate that many biological energy converters may have managed to prolong the domain of linear laws between flows and forces into the far-from-equilibrium regime by virtue of their evolutionary drive towards higher efficiency.

Acknowledgements

The authors would like to thank to Professors T.L. Hill and G. Nicolis for stimulating discussions. One of us (J.W.S.) would also like to acknowledge his gratitude to the late Dr. M. Berman for making possible a brief visit to the National Institutes of Health, Bethesda, MD, where this study was initiated. This work was supported by the Swiss National Science Foundation.

References

1 H. Rottenberg, Biochim. Biophys. Acta 549 (1979) 225.
2 J.W. Stucki, Eur. J. Biochem. 109 (1980) 269.
3 J.J. Lemasters and W.H. Billica, J. Biol. Chem. 256 (1981) 12949.
4 M.A. Lang, S.R. Caplan and A. Essig, J. Membrane Biol. 31 (1977) 19.
5 S.R. Caplan and A. Essig, Curr. Top. Membranes Transp. (1977) 145.
6 I. Prigogine, Introduction to thermodynamics of irreversible processes (John Wiley, New Yor, 1967).
7 A. Katchalsky and P. Curran, Nonequilibrium thermodynamics in biophysics (Harvard University Press, Cambridge, MA, 1965).
8 T.L. Hill, Free energy transduction in biology (Academic Press, New York, 1977).
9 G. von Jagow and W.D. Engel, Angew. Chem. Int. Ed. 19 (1980) 659.
10 D. Walz, Biochim. Biophys. Acta 505 (1979) 279.
11 O. Kedem and S.R. Caplan, Trans. Faraday Soc. 21 (1965) 1897.
12 M. Compiani, EBEC Rep. 2 (1982) 527.
13 P. Glansdorff and I. Prigogine, Thermodynamic theory of structure, stability and fluctuation (John Wiley, New York, 1971).
14 G. Nicolis and I. Prigogine, Self-organization in nonequilibrium systems (John Wiley, New York, 1977).
15 J.W. Stucki, Eur. J. Biochem. 109 (1980) 257.
16 A. Essig and S.R. Caplan, Proc. Natl. Acad. Sci. U.S.A. 78 (1981) 1647.
17 W. Nagel and A. Essig, J. Membrane Biol. 69 (1982) 125.